

## Nonexistence of the decahedral $\text{Si}_{20}\text{H}_{20}$ cage: Levinthal's paradox revisited

Deb Sankar De <sup>1</sup>, Bastian Schaefer,<sup>1</sup> Bernd von Issendorff,<sup>2</sup> and Stefan Goedecker<sup>1</sup>

<sup>1</sup>*Department of Physics, Universität Basel, Klingelbergstr. 82, 4056 Basel, Switzerland*

<sup>2</sup>*Department of Physics, Universität Freiburg, Hermann-Herder-Str. 3, 79104 Freiburg, Germany*



(Received 18 January 2020; accepted 23 April 2020; published 1 June 2020)

The decahedral cage is the theoretically established ground state of the hydrogen saturated  $\text{Si}_{20}\text{H}_{20}$  fullerene. However it has never been observed experimentally. Based on an extensive exploration of the potential energy surface and by constructing theoretical reaction pathways from possible initial structures to the ground state of  $\text{Si}_{20}\text{H}_{20}$ , we show that there is no driving force towards the global minimum. There exists a huge number of intermediate structures that consist mainly of collapsed cages. Visiting all these intermediate states to find the ground state is not possible on experimentally relevant time scales. In this way the ground state becomes kinetically inaccessible. We contrast the features of the potential energy landscape of  $\text{Si}_{20}\text{H}_{20}$  with that of  $\text{C}_{60}$  which spontaneously forms by condensation.

DOI: [10.1103/PhysRevB.101.214303](https://doi.org/10.1103/PhysRevB.101.214303)

### I. INTRODUCTION

Condensed matter systems can adopt a huge number of structures. This comes from the fact that the potential energy function has an equally large number of local minima, each of which corresponds to a metastable structure. Bulk materials can for instance be found in a huge number of amorphous structures, clusters in a very large number of isomers, and biomolecules in an astronomically large number of conformers. It is at present not fully understood which structure out of this huge number of theoretically possible structures can really be found in nature. This problem has extensively been discussed in the context of protein folding. The number of possible conformers grows exponentially with the number of residues. However only one configuration out of this exponentially large number of possible conformations, the configuration with the lowest free energy, is formed by a folding mechanism in living organisms and can perform its required biological role. Based on a simple estimate of the time required to jump from one intermediate structure into another one, Levinthal [1] argued that the folding, i.e., the time to arrive at its correct ground state, should require a time longer than the age of the universe, even if only a small fraction of all possible configurations has to be visited as intermediates along the reaction pathway describing the folding. Since it is however experimentally well established that proteins do fold on a quite short time scale, these arguments are known as the Levinthal paradox. The Levinthal paradox was resolved by the folding funnel hypothesis [2] which shows that on a funnel like potential energy surface the system can fall into the ground state at the bottom of the funnel along a reaction pathway that contains only a modest number of intermediate states. This is possible because the reaction pathway is embedded in some low-dimensional manifold of the funnel, whereas the entire funnel is a high-dimensional object in configuration space that consequently contains an exponentially large number of local minima. In order to establish such a short reaction pathway, it is however necessary to have a

strong driving force towards the global minimum. Such a driving force gives rise to a reaction pathway whose downhill barriers are systematically lower than the uphill barriers. By definition the downhill barrier is the barrier that the system has to overcome when it jumps from one intermediate state into another one that is lower in energy, whereas the uphill barrier is the one that has to be overcome when it jumps into a higher energy state. In this way a strong directionality or driving force towards the global minimum is imposed since, according to standard transition state theory, it is more likely to cross low barriers than high barriers. It is widely believed that those proteins that have such a strong directionality were selected during the biological evolution of life because they can rapidly fold into a well defined functional structure.

A fundamental question that we want to answer is whether a nanosystem with a well defined ground state will necessarily have such a funnel-like structure that will ensure that it will form quasiautomatically by some kind of physical self assembly process on a short time scale or whether, on the contrary, there exist systems whose ground state is virtually not accessible by a short directional reaction pathway on a reasonable time scale. As an example we will study the hydrogen saturated  $\text{Si}_{20}\text{H}_{20}$  fullerene.

Nanosciences requires building blocks on the nanometer scale with a large variety of properties. Carbon-based nanostructures such as fullerenes, nanotubes, nanosheets, and carbon based polymers are common building blocks [3–5]. Some similar structures do exist for Si as well, namely linear polysilanes, silicon nanosheets, and nanotubes [6,7], but silicon fullerenes have not been found so far. While carbon atoms can readily adjust their valence states to participate in single, double, and triple bonds, silicon strongly prefers  $sp^3$  hybridization and single bonds. Therefore, although  $\text{C}_{20}$  is the lowest stable fullerene structure, quantum chemical calculations show the  $\text{Si}_{20}$  fullerene to be highly unstable [8].

The stability of a cage structure can be enhanced by various modifications. One theoretically proposed possibility is

endohedral doping with a metal atom which fills the  $\text{Si}_{20}$  cluster cavity [9]. However unbiased structure predictions have shown that this strategy frequently fails and other noncage structures are significantly lower in energy [10]. A second approach is to exohedrally passivate the dangling bonds of the Si atoms in the  $\text{Si}_{20}\text{H}_{20}$  dodecahedron by hydrogen attachment. The resulting dodecahedral configuration has theoretically been proposed as the global minimum of  $\text{Si}_{20}\text{H}_{20}$  [11–13]. Even though we also performed extensive structural searches in this study we were not able to find any lower energy structure. The third, hybrid approach combines both ideas to obtain stable endohedrally doped  $X@Si_{20}H_{20}$ , where  $X$  is a metal/halide [13–15]. So even though it is firmly established that the dodecahedral  $\text{Si}_{20}\text{H}_{20}$  fullerene is the ground state structure, no experimental evidence for the existence of this hydrogen saturated fullerene is present to the best of the authors' knowledge. The structure of smaller silicon hydrogen clusters has been studied and complex 3-center 2-electron Si-H-Si bonds were found [16].

The question of whether the ground state of clusters is only determined by equilibrium thermodynamics or whether kinetic effects can also play an important role is a long standing one. In this work, we show that kinetic effects are very important in the  $\text{Si}_{20}\text{H}_{20}$  fullerene and we explain why the dodecahedral ground state configuration of  $\text{Si}_{20}\text{H}_{20}$  was never observed in experiment. We demonstrate that the potential energy surface of  $\text{Si}_{20}\text{H}_{20}$  has striking differences compared to the potential energy surfaces of the easily synthesizable  $\text{C}_{60}$  cluster.

As tools to understand the dynamical behavior of our clusters we calculate reaction pathways and construct disconnectivity graphs. A disconnectivity graph [17] is a powerful tool to understand the characteristics of a potential energy surface. Each lower end (leaves) of the graph represents a local minimum, and its height shown along the  $y$  axis gives the energy of this minimum. The highest point of the path connecting two minima in a disconnectivity graph gives an energy window for the height of the highest barrier that has to be surmounted in a transformation from one minimum into another one along the lowest energy pathway, so it is the lowest highest barrier. This barrier will be called in the following the accumulated barrier height. In a complex reaction pathway such a transformation from an initial into a final minimum overcomes in general multiple barriers. The accumulated barrier height does not contain information about the height of all these individual barriers along the transformation pathway. We just indicate the highest one.

## II. COMPUTATIONAL METHODOLOGY

Our investigation required the calculation of a huge number of local minima and saddle points. Force field methods do not give a reliable description of the potential energy surface [18], whereas density functional calculations would have been too expensive. The potential energy surface was therefore explored using a self-consistent charge density functional tight-binding method (SCC-DFTB) with  $s$  and  $p$  atomic orbitals for silicon and an  $s$  orbital for hydrogen. The parameters were fitted to reproduce standard DFT results with the Perdew-

Burke-Ernzerhof PBE functional [19]. This turns out to be a good compromise between speed and accuracy. The accuracy of the DFTB approximation for  $\text{Si}_{20}\text{H}_{20}$  has been assessed by a comparison with DFT calculations performed with BIGDFT [20] using the same functional and NLCC dual space Gaussian pseudopotentials [21]. The very good agreement between DFT and DFTB energies for a subset of 2000 structures is shown in the Supplemental Material (SM) [22]. In particular there is good agreement for the height of the barriers that are a central quantity in this work. The barrier height between the ground state and the second lowest minimum [a structure with one Stone-Wales (SW) defect] of  $\text{C}_{60}$  is 0.25 Ha) in DFTB whereas it is (0.27 Ha) in DFT [23,24] with the PBE functional [25]. Barrier heights obtained from DFT calculations were shown to agree well with the ones obtained from higher level calculations [18] for rearrangement processes in silicon clusters. Geometry optimizations were considered converged after reaching a maximal force component on any atom smaller than  $1 \times 10^{-5}$  eV Å.

The unbiased search of new configurations was performed by employing the minima hopping (MH) method [26]. MH can efficiently search low-energy structures by exploiting the Bell-Evans-Polanyi principle for molecular dynamics [27,28]. This method has been successfully used to efficiently locate the lowest energy minima in a large variety of applications [29–35].

The transformation pathways were found by the minima hopping guided path search (MHGPS) [36] in case of  $\text{C}_{60}$  where no bias is necessary to find the ground state. Exploiting information from the MD trajectories that connect different local minima in a MH run, the algorithm locates the transition states (saddle point) located between two input configurations visited consecutively in a MH run. The transition states of the  $\text{C}_{60}$  molecule are then found by a stabilized quasi-Newton method [37]. Two local geometry optimizations are subsequently performed after displacing the system away from the saddle point by a small positive and negative step size along the direction of the eigenvectors of the Hessian matrix with negative curvature. In case these minima do not correspond to the initial input structures, the procedure is repeated recursively until they are found. All the minima and transition states that emerge from these connection attempts form a stationary point database consisting of all pairs of minima together with their connecting saddle point. From this database the lowest energy pathways can be extracted by the Dijkstra algorithm [38]. The final results can be visualized as a disconnectivity graph [17]. The graphs in our study were created using the disconnectionDPS software [39].

In case of  $\text{Si}_{20}\text{H}_{20}$  where a bias is needed to find a transformation pathway that leads into the ground state, our approach was identical except that the biased minima hopping guided path search (BMHGPS) [40] was used to find the transformation pathway. In this method the dodecahedral configuration of  $\text{Si}_{20}\text{H}_{20}$  is pulled down energetically with respect to the other structures, such that it can be reached more easily. The heights of the barriers that are not along the reaction pathway were obtained by a fingerprint-based extrapolation scheme [41]. Both for this scheme and the biasing an overlap matrix based fingerprint with  $s$  and  $p$  orbitals [42] was used. An

additional bias was obtained by putting a repulsive Lennard Jones atom in the center of the cluster. This penalized the undesired collapse of the cage.

The same fingerprint was also used to calculate the distance-energy (DE) plots [43]. In a DE plot the fingerprint distance from the ground state is plotted along the  $x$  axis and the energy relative to the ground state along the  $y$  axis for a large collection of metastable structures. The slope of this plot indicates how much energy can be gained when the structure becomes more similar to the ground state and shows therefore also the strength of the driving force toward the ground state.

### III. RESULTS AND DISCUSSIONS

In order to better understand the particular features of the PES of Si<sub>20</sub>H<sub>20</sub> we contrast it with a system that can easily be grown, namely C<sub>60</sub>. We analyze three different quantities to describe the features of the potential energy surface of these two systems: Disconnectivity graphs, reaction pathways, and DE plots.

#### A. C<sub>60</sub>

Disconnectivity graphs for C<sub>60</sub> have been calculated previously [24] for a subset of structures that are connected through pyracylene rearrangements [44] which exchange hexagons and pentagons. Our search in contrast does not contain any constraints and one finds numerous structures with four member and seven member carbon rings. Some of these structures that give rise to some secondary funnels are shown in Fig. 1. Previous simulations suggest that such configurations play an important role in fullerene formation [45,46]. The reaction pathway for the transformation of a Stone-Wales defect into the ground state has also been studied at various levels of theory [25] and agrees with our findings. To construct the fingerprint (FP)-based disconnectivity graph represented in Fig. 1 we considered 10 000 different C<sub>60</sub> configurations, with almost all structures visited at least twice in a minima hopping run. This suggests a quite complete sampling of the configurations within the energy range of the disconnectivity graph of 0.8 Ha. In spite of these differences in the data set used for the construction, our disconnectivity plot agrees qualitatively with the one from a previous study [24]. The disconnectivity graph (Fig. 1) is of the weeping willow type [47]. The global minimum of C<sub>60</sub>, the fullerene cage, is at the bottom of a very large funnel that goes up some 0.8 Ha in energy. All the structures in this funnel are cagelike but contain more and more defects as one goes up in energy. The driving force toward the global minimum is clearly visible in the DE plot (Fig. 2). In this whole energy range there are no fragmented structures.

In agreement with a previous study [48] our MD runs for C<sub>60</sub> show from 3800 K on a diffusive motion which leads to extensive isomerization and can be considered as an indication of an upcoming melting process. To study the formation of C<sub>60</sub> we will go to a somewhat lower temperature of 3500 K, where the Boltzmann probability of finding the ground state is already about 99% (see Fig. 3).

Since there is already a natural bias toward the ground state, MH runs can find the ground state without the need

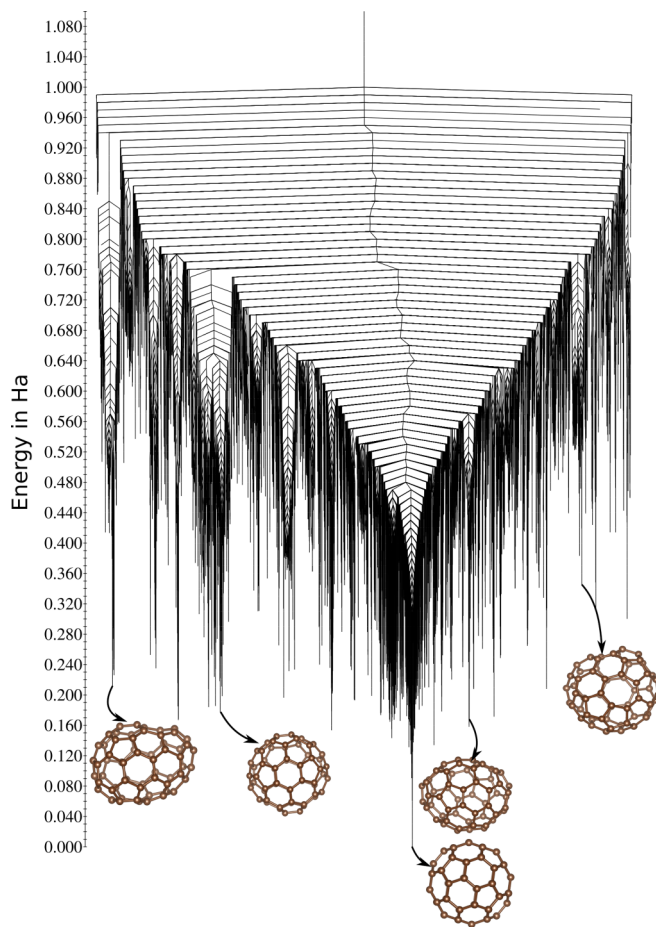


FIG. 1. Disconnectivity plot of C<sub>60</sub>. The structures at the bottom show the lowest energy configuration of some selected superbases.

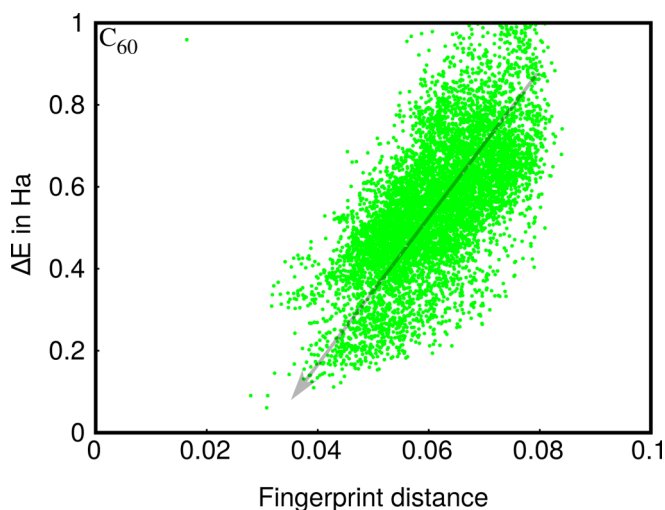


FIG. 2. DE plot of C<sub>60</sub>. For any structure one can find another structure that is more similar to the ground state and that is in nearly all cases lower or in a few cases slightly higher in energy. Hence one gains quasicontinuously energy by moving toward the ground state. The arrow is meant as a guide to the eye, visualizing the average driving force.

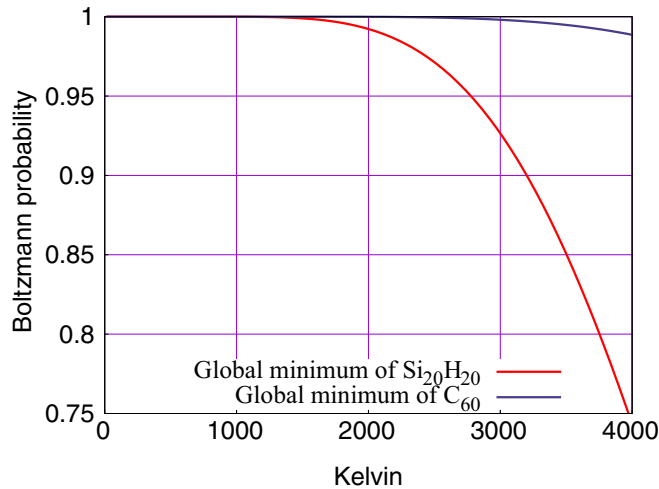


FIG. 3. The Boltzmann probability for finding the ground state as a function of temperature.

of any additional bias. The driving force is clearly visible in all the transformation pathways that we found for  $C_{60}$  (see Fig. 4). The downhill barriers are on average systematically lower than the uphill barriers which is visible as some downward trend of the pathway. Since the barriers of about 0.2 Ha are quite high compared to  $k_B T$  at room temperature (which corresponds to 0.001 Ha), high temperature is needed. But at these high temperatures, the cluster is a structure seeker [24]. Let us now study the dynamics of  $C_{60}$  at an annealing temperature of 3500 K. At this temperature the barriers can be overcome on a time scale of  $10^{-6}$  sec according to standard transition state theory. Since for a typical reaction pathway some 20 barriers have to be crossed the time scale of formation of  $C_{60}$  is about  $2 \times 10^{-5}$  sec. As typical formation

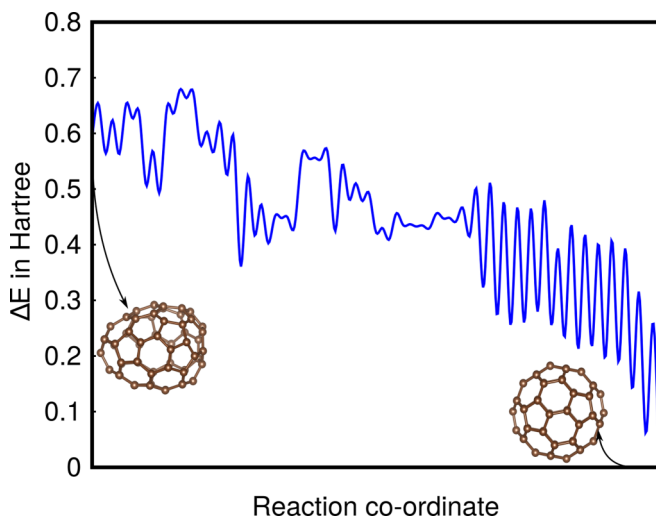
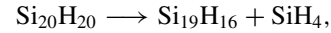
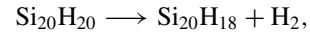


FIG. 4. Lowest barrier transformation path from a defective cage to the  $C_{60}$  fullerene ground state. More such transformation pathways are shown in the SM. All these transformation pathways have in common that there is a clear downward trend visible. Only in the first part of the transformation some of the path has to climb up to escape from some superbasin.

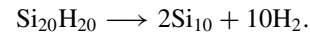
times in laser evaporation sources are on the order of tens to hundreds of microseconds, it seems therefore reasonable that  $C_{60}$  fullerene can be preferentially formed. There is no definite information available about the cluster temperatures in such laser evaporation sources.

### B. $Si_{20}H_{20}$

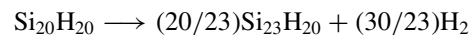
Let us now turn to  $Si_{20}H_{20}$ . We first verified that the system is stable with respect to various plausible decompositions such as



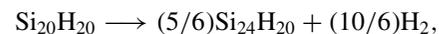
and



The last decomposition was motivated by the fact that the  $Si_{10}$  ground state is particularly stable [49]. By performing a MH based structure prediction for  $Si_{20}H_{18}$  and  $Si_{19}H_{16}$  we found that these decompositions are endothermic requiring, respectively, an energy of 0.06, 0.11, and 0.45 Ha. Forming  $Si_{20}H_{20}$  out of bulk Si and  $H_2$  molecules requires a relatively small energy of 0.11 Ha compared to the case of  $C_{60}$  where 1.24 Ha are required to form it out of graphene. The lowest energy configurations of these clusters are given in the SM. Hydrogen depleted Si clusters, where the number of Si atom is more than 22 [50], are observed in experiment at low temperatures. We therefore also investigated the possibility of decomposition of  $Si_{20}H_{20}$  clusters into bigger clusters, i.e.,  $Si_{23}H_{20}$  and  $Si_{24}H_{20}$ . We started MH calculations for these clusters and we observed that the lowest energy configurations consist of cages that are stabilized by stuffing with additional silicon atoms. This is in agreement with experimental observations [50]. Our theoretical structures are again given in the SM. We found that both the decompositions from  $Si_{20}H_{20}$  to  $H_2$  and  $Si_{23}H_{20}$  and  $Si_{24}H_{20}$ ,



and



are endothermic requiring energies of 2.67 Ha and 0.73 Ha.

So  $Si_{20}H_{20}$  is on the convex hull of all reasonable decompositions. For this reason we will concentrate in our simulations onto unfragmented structures of  $Si_{20}H_{20}$ . Whenever a fragmentation occurs our algorithm will try to reassemble the fragments into a cluster.

The first metastable structure (shown in the SM) is a cage where one hydrogen is inside the cage. Like all the other hydrogens that are outside the cage it is bonded to one silicon. This structure is energetically well separated from the ground state by 0.034 Ha. We have also found other cage and non-cage-like metastable configurations and different types of bonding between Si and H (shown in SM) [16].

The first striking difference between the potential energy surface of  $Si_{20}H_{20}$  and the previously studied  $C_{60}$  is that the density of structures is much higher. In the energy window defined by the energies of our initial structures and the ground state of  $Si_{20}H_{20}$  we found 55 000 structures. Even though

this number is about five times larger than the number of structures that we have generated for  $\text{C}_{60}$ , we certainly have not completely sampled the potential energy surface. Based on an analysis of the probabilities for visiting a certain structure twice (see SM), we estimate that our data base contains only about a quarter of all possible structures and that there exist about 200 000 structures in this energy range. It has to be pointed out that this huge number of structures exists in an energy interval that is about three times smaller than the one considered in the case of  $\text{C}_{60}$ . Silicon clusters can fragment before they melt [49]. We found the same behavior for  $\text{Si}_{20}\text{H}_{20}$ . Our MD simulations show indications of melting at about 1700 K for  $\text{Si}_{20}\text{H}_{20}$  and so we consider 1500 K as the highest possible annealing temperature. Figure 3 shows at this temperature the probability to find the ground state is more than 99%. Such high temperatures will however not be observed during growth. As we have seen, the attachment of a  $\text{H}_2$  molecule liberates an energy of 0.06 Ha and the attachment of a  $\text{SiH}_4$  unit 0.11 Ha. Within classical thermodynamics, dissipating these two energies into heat will rise the temperature by about 150 and 300 K. In a quantum mechanical treatment the silicon hydrogen stretch vibrations would be frozen out in this temperature range and the temperature increase would be about 20 percent larger.

In our calculations of reaction pathways into the global minimum we used a few starting configurations. One was the ground state of the  $\text{Si}_{20}$  cluster [51] whose surface was saturated with 20 hydrogen. This initial structure is 0.23 Ha above the ground state. The other configurations were lowest energy configurations of randomly selected different superbases in Fig. 5 whose energy was about 0.055 Ha above the ground state.

Running a standard MH from various starting configurations we were not able to find the ground state unless we started in the red superbasin of Fig. 5. This can be understood from the DE plot of Fig. 6. As indicated by the arrow in this figure, there is a strong driving force towards low-energy configurations with a fingerprint distance between 0.06 and 0.08. As a matter of fact all the minima hopping runs that failed to find the global minimum ended up in this region of the DE plot. A driving force that would drive the system from this region toward the ground state does not exist.

The disconnectivity graph of Fig. 5 resembles a banyan tree [47] due to its self-similar features. Hence there are glassy regions without any driving force towards a certain structure and the superbases act as traps in the evolution of the system towards the ground state. This can also be understood by geometric arguments. In contrast to  $\text{C}_{60}$  where all the low-energy structures are cagelike structures, most structures of  $\text{Si}_{20}\text{H}_{20}$  are not cagelike. If one has now by chance a cagelike structure there is a huge number of transformations that destroy the cage but only very few that leave the cage intact and that might therefore lead to the ground state.

As can be seen from Fig. 5, downhill and uphill barriers are mostly of comparable height and are peaked around 0.04 Ha. This is much smaller than a typical accumulated barrier height which is about 0.2 Ha (Fig. 5).

A driving force towards the ground state can however be obtained in a simulation by adding a permutationally invariant bias [40] (see SM) to the physical potential energy surface that

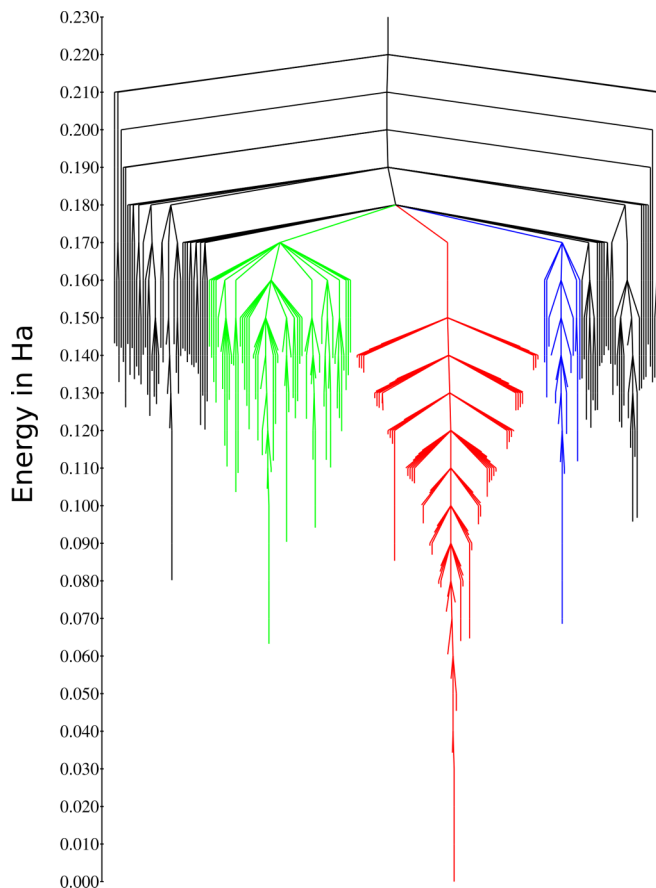


FIG. 5. Disconnectivity plot for  $\text{Si}_{20}\text{H}_{20}$  based on 500 lowest energy configurations. The configurations colored in green represent the biggest superbasin, with  $\approx 220$  structures. The global minimum belongs to the superbasin colored in red, that contains 100 structures. The superbasin with blue color has 50 configurations. Because of the much higher configurational density of states of  $\text{Si}_{20}\text{H}_{20}$ , a much smaller energy interval has to be selected compared to  $\text{C}_{60}$  in order to obtain a graph where the individual branches can still be resolved visually.

pulls the system towards its ground state. This bias transforms a glassy potential energy surface into the potential energy surface of a structure seeker, i.e., the downhill barriers that lead towards the ground state are lowered with respect to the uphill barriers and therefore the system is likely to move toward the global minimum. As has been shown already for proteins a quite small bias of the order a few  $k_B T$  is sufficient to obtain this effect [52]. The problematic region in the DE plot of the physical potential energy surface (region in Fig 6 with energies below 0.1 Ha) is strongly modified by the bias and shows a clear driving force towards the ground state as shown in Fig. 7. In this way we could find for all starting configurations reaction pathways leading to the ground state. One representative pathway, transformed back on the physical potential energy surface, is shown in Fig. 8. Several more such pathways are shown in the SM. They have all in common that they traverse a broad flat region and that there is only a clear driving force toward the global minimum in the very last part of the reaction pathway.

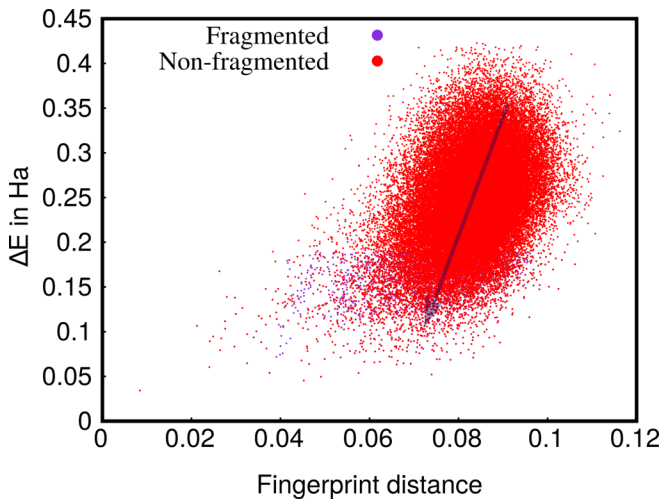


FIG. 6. Distance energy (DE) plot of  $\text{Si}_{20}\text{H}_{20}$  clusters. The fingerprint distances and energy differences are calculated with respect to the ground state configuration. The plot is based on 55 000 nonfragmented low-energy configurations. A very small and entirely incomplete set of very low-energy fragmented structures is also included to illustrate their region of existence in the DE plot. The lowest fragment is about 0.07 Ha above the ground state. The arrow is meant as a guide to the eye to visualize the driving force, which in this case does not point toward the ground state.

It is extremely unlikely that the real physical system will follow such a reaction pathway found in the biased simulation. At each intermediate state the system has the possibility to cross over some 10 barriers of comparable height into other local minima that are not on the reaction pathway (for details see Fig. 6 in SM). For the shortest reaction pathway we found that there are already some 20 intermediate states. Hence, the probability to follow this reaction pathway is about  $10^{-20}$ . So

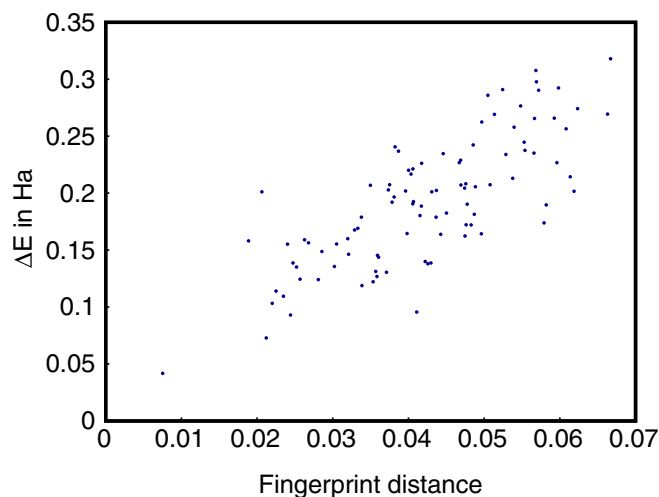


FIG. 7. DE plot of the biased potential energy surface. It is shown only for the configurations in the region where there was no driving force toward the global minimum in the original unbiased DE plot. The bias magnifies the energy differences between configurations that are not similar to the ground state and induces in this way a driving force towards the targeted configuration.

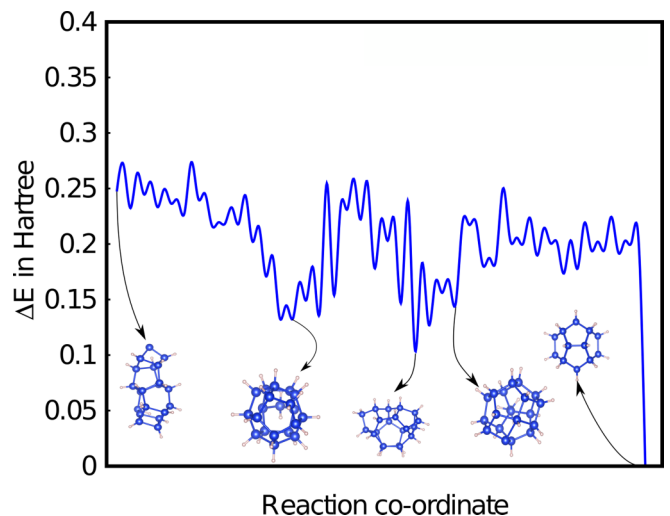


FIG. 8. A possible reaction pathway path from the hydrogenated  $\text{Si}_{20}$  global minimum structure of  $\text{Si}_{20}$  to the dodecahedron  $\text{Si}_{20}\text{H}_{20}$  ground state configuration found by BMHPGS. The shown energies are the energies from the physical potential energy surface without the bias.

the real physical system will get kind of lost in these glassy regions of the PES and not reach the global minimum on a reasonably short time scale.

If there is no funneling on the physical PES towards the ground state, we have to evoke the arguments by Levinthal, i.e., the system has to visit a considerable fraction of all its local minima before it will fall into its ground state. Experimentally hydrogenated silicon clusters have been generated in a magnetron gas aggregation cluster source (see SM) performed in the laboratory of Prof. Issendorff. To get the fastest possible relaxation time we will first assume that we have the highest possible temperature of about 1500 K. In the experimental setup, the clusters are cooled down from an initial temperature by collisions with a buffer gas to a temperature of some 100 K on a time scale of about  $1 \times 10^{-5}$  sec. At this low temperature structural rearrangements are not possible any more. So the ground state has to be found within this annealing time and we assume that the temperature will be constant at 1500 K during this annealing process. As can be seen either from the disconnectivity graph [Fig. 5 or our reaction pathway (Fig. 6 in SM)] there are numerous barriers with a height of about at least 0.08 Ha that have to be crossed to reach the ground state. These barriers typically separate different superbasins. Within a superbasin the barriers are lower and the dynamics can be quite fast. Let us now assume that we have  $M$  superbasins each containing on average  $n$  local minima such that the total number of local minima  $N$  is given by  $N = Mn$ . Standard transition state theory gives an attempt frequency of  $i\omega_A = k_B T / \hbar = 3 \times 10^{13}$ /sec at 1500 K. If one tries to jump out of a superbasin, most jumps will however occur within the superbasin and the probability for trying to jump out of the superbasin will be reduced by  $1/n$ . To visit all the  $M = N/n$  superbasins would then take  $(M/(\omega_A/n)) \exp(0.08/0.0048) = (N/(\omega_A)) \exp(0.08/0.0048)$ . Here 0.08 Ha is the average barrier height from our reaction pathways and  $k_B T = 0.0048$  Ha at  $T = 2000$  K. The numerical value for this expression is

0.1 sec for  $N = 200\,000$ . In current experimental set-ups, the temperature will however be much lower than 1500 K. As we have shown before a typical attachment rises the temperature of the cluster by about 300 K. So if the temperature of the cooling gas is about 100 K, the resulting temperature will be about 400 K. In this case overcoming one single barrier of height 0.08 Ha will take  $1 \times 10^{14}$  sec. Since all these times are significantly longer than the anneal time,  $\text{Si}_{20}\text{H}_{20}$  will not form.

In addition to the annealing, there is still another even faster process which will further reduce the likelihood of finding the ground state  $\text{Si}_{20}\text{H}_{20}$  icosahedron. As was pointed out before we suppress in our MH simulation the fragmentation of the cluster. To overcome this limitation, we performed MD simulations at the highest possible temperature that would result in the fastest relaxation into the ground state, namely 1500 K. In these simulations of  $\text{Si}_{20}\text{H}_{20}$  we could very frequently observe fragmentations after a few hundred picoseconds of simulation time and  $\text{H}_2$  molecules with  $\text{Si}_{20}\text{H}_{18}$  clusters were the most common fragments formed. In contrast to  $\text{C}_{20}\text{H}_{18}$  the ground state of  $\text{Si}_{20}\text{H}_{18}$  (shown in the SM) is not a dodecahedron cage or a slightly distorted version of such a cage but a collapsed cage with a reduced surface area. In order to form again a  $\text{Si}_{20}\text{H}_{20}$  cluster the  $\text{H}_2$  molecule has to hit a place on the surface of some configuration of  $\text{Si}_{20}\text{H}_{18}$  where two undercoordinated silicon atoms are located. We were not able to observe a single event of this type in standard molecular dynamics runs. Only by preparing by hand  $\text{H}_2$  trajectories that hit exactly the reactive spot on a selected cluster such an event could be observed. If the rates of the forward and backward reaction are so different, it follows from the principle of detailed balance that the equilibrium population of  $\text{Si}_{20}\text{H}_{20}$  is small compared to the population of other products which are easily formed during MD runs. This is actually confirmed by an experimental analysis of the mass spectra of hydrogenated silicon clusters produced in a magnetron sputter source (see SM). There is a broad distribution of  $\text{Si}_{20}\text{H}_x$  where  $x$  ranges from 0 to about 30, with a peak around  $x = 18$ . In summary, this means that first of all it is very unlikely to encounter in a silicon hydrogen system with the overall correct one-to-one stoichiometry a cluster that has exactly 20 silicon and 20 hydrogen atoms. In the rare cases where such a cluster is created, it will not be able to fall fast enough into its ground state before it undergoes further fragmentation or fusion events that change the stoichiometry.

In the epilogue of our study we will now discuss under what experimental conditions related structures might be synthesized. The main reason for the absence of any funneling tendency toward the dodecahedron ground state cage structure was the fact that a huge number of collapsed cage structures exist that are nearly degenerate in energy and that there was a strong tendency for hydrogen detachment. The tendency for detachment could be reduced by stronger bonds. Silicon fluorine and silicon chlorine bonds are much stronger than silicon hydrogen bonds. For both elements the dodecahedron

is a stable structure but surprisingly it turns out that it is not the ground state. Structures with a collapsed cage are lower in energy for both elements. The numerical bias that we used in our minima hopping simulation penalized structures that have atoms inside the desired cage structure and prevented thus a collapse of the cage. Something similar has been done in the synthesis of  $[\text{Si}_{32}\text{Cl}_{45}]^-$  [53], the only known cluster that contains a 20 atom silicon cage. In this cluster a central  $\text{Cl}^-$  ion inside the  $\text{Si}_{20}$  cage prevents the collapse of the cage.

In materials sciences the general belief is that only well defined structures can perform a specific function. The same belief was prevailing in biology for a long time concerning proteins. Things have however changed with the discovery of intrinsically disordered proteins, which do perform many biologically important processes [54]. In the same way it might turn out that some fluctuating structures such as  $\text{Si}_{20}\text{H}_{20}$  could be useful in some context.

#### IV. CONCLUSIONS

Our results show that it is very unlikely that  $\text{Si}_{20}\text{H}_{20}$  can be formed experimentally by a simple condensation type of process that allows for instance for the synthesis of  $\text{C}_{60}$ . It would be necessary that this condensation occurs on a time scale which is small compared to other relevant time scales, namely the annealing time scale and the time scale for competing processes such fragmentation or fusion. The different behavior of  $\text{C}_{60}$  and  $\text{Si}_{20}\text{H}_{20}$  results from the different nature of their potential energy surfaces. Whereas for  $\text{C}_{60}$  there exist many reaction pathways that lead downwards in the big funnel of all cagelike structures towards the ground state and show therefore a clear driving force toward the global minimum, such reaction pathways do not exist for  $\text{Si}_{20}\text{H}_{20}$ . Such reaction pathways would however be necessary in order to form rapidly the icosahedron ground state once a short lived cluster with the right  $\text{Si}_{20}\text{H}_{20}$  stoichiometry is generated.

Whereas state of the art structure prediction methods [55] allow us to find the ground state and metastable structures on the potential energy surface, our work shows that the recently proposed BMHGPS method, that is rooted in the MH structure prediction method, allows us to go one step further and to understand also the dynamics of the system on this potential energy surface. In this way conclusions about the synthesizability of a system can be drawn.

#### ACKNOWLEDGMENTS

This was supported by the NCCR MARVEL, funded by the Swiss National Science Foundation. Computational resources provided by the Swiss National Supercomputing Center (SCS) in Lugano under the projects s707 and s963 are gratefully acknowledged. Calculations were also performed at the sciCORE [56] scientific computing core facility at the University of Basel.

[1] C. Levinthal, in *Mossbauer Spectroscopy in Biological Systems: Proceeding of a Meeting Held at Allerton House*, edited by

J. T. P. De Brunner and E. Munck (University of Illinois Press, Monticello, Illinois, 1969), pp. 22–24.

- [2] K. A. Dill and H. S. Chan, *Nat. Struct. Biol.* **4**, 10 (1997).
- [3] H. W. Gibson, R. J. Weagley, R. A. Mosher, S. Kaplan, W. M. Prest, and A. J. Epstein, *Phys. Rev. B* **31**, 2338 (1985).
- [4] K. S. Novoselov, A. K. Geim, S. V. Morozov, D. Jiang, M. I. Katsnelson, I. V. Grigorieva, S. V. Dubonos, and A. A. Firsov, *Nature (London)* **438**, 197 (2005).
- [5] P. Boul, J. Liu, E. Mickelson, C. Huffman, L. Ericson, I. Chiang, K. Smith, D. Colbert, R. Hauge, J. Margrave, and R. Smalley, *Chem. Phys. Lett.* **310**, 367 (1999).
- [6] R. D. Miller and J. Michl, *Chem. Rev.* **89**, 1359 (1989).
- [7] H. Okamoto, Y. Kumai, Y. Sugiyama, T. Mitsuoka, K. Nakanishi, T. Ohta, H. Nozaki, S. Yamaguchi, S. Shirai, and H. Nakano, *J. Am. Chem. Soc.* **132**, 2710 (2010).
- [8] K.-M. Ho, A. A. Shvartsburg, B. Pan, Z.-Y. Lu, C.-Z. Wang, J. G. Wacker, J. L. Fye, and M. F. Jarrold, *Nature (London)* **392**, 582 (1998).
- [9] Q. Sun, Q. Wang, T. M. Briere, V. Kumar, Y. Kawazoe, and P. Jena, *Phys. Rev. B* **65**, 235417 (2002).
- [10] A. Willand, M. Gramzow, S. Alireza Ghasemi, L. Genovese, T. Deutsch, K. Reuter, and S. Goedecker, *Phys. Rev. B* **81**, 201405(R) (2010).
- [11] C. W. Earley, *J. Phys. Chem. A* **104**, 6622 (2000).
- [12] A. D. Zdetsis, *Phys. Rev. B* **76**, 075402 (2007).
- [13] D. Palagin and K. Reuter, *Phys. Rev. B* **86**, 045416 (2012).
- [14] C.-Y. Zhang, H.-S. Wu, and H. Jiao, *Chem. Phys. Lett.* **410**, 457 (2005).
- [15] F. Pichierri, V. Kumar, and Y. Kawazoe, *Chem. Phys. Lett.* **406**, 341 (2005).
- [16] M. A. R. George and O. Dopfer, *Int. J. Mass Spectrom.* **435**, 51 (2019).
- [17] O. M. Becker and M. Karplus, *J. Chem. Phys.* **106**, 1495 (1997).
- [18] S. A. Ghasemi, M. Amsler, R. G. Hennig, S. Roy, S. Goedecker, T. J. Lenosky, C. J. Umrigar, L. Genovese, T. Morishita, and K. Nishio, *Phys. Rev. B* **81**, 214107 (2010).
- [19] J. P. Perdew, K. Burke, and M. Ernzerhof, *Phys. Rev. Lett.* **77**, 3865 (1996).
- [20] L. Genovese, A. Neelov, S. Goedecker, T. Deutsch, S. A. Ghasemi, A. Willand, D. Caliste, O. Zilberberg, M. Rayson, A. Bergman, and R. Schneider, *J. Chem. Phys.* **129**, 014109 (2008).
- [21] A. Willand, Y. O. Kvashnin, L. Genovese, A. Vazquez Mayagoitia, A. K. Deb, A. Sadeghi, T. Deutsch, and S. Goedecker, *J. Chem. Phys.* **138**, 104109 (2013).
- [22] See Supplemental Material at <http://link.aps.org/supplemental/10.1103/PhysRevB.101.214303> for DFT and DFTB co-relation plot, different reaction pathways, different transition states, mass spectra of Si<sub>20</sub>H<sub>20</sub> and different structures of Si<sub>m</sub>H<sub>n</sub> clusters.
- [23] Y. Kumeda and D. J. Wales, *Chem. Phys. Lett.* **374**, 125 (2003).
- [24] T. R. Walsh and D. J. Wales, *J. Chem. Phys.* **109**, 6691 (1998).
- [25] H. F. Bettinger, B. I. Yakobson, and G. E. Scuseria, *J. Am. Chem. Soc.* **125**, 5572 (2003).
- [26] S. Goedecker, *J. Chem. Phys.* **120**, 9911 (2004).
- [27] S. Roy, S. Goedecker, and V. Hellmann, *Phys. Rev. E* **77**, 056707 (2008).
- [28] M. Sicher, S. Mohr, and S. Goedecker, *J. Chem. Phys.* **134**, 044106 (2011).
- [29] D. S. De, J. A. Flores-Livas, S. Saha, L. Genovese, and S. Goedecker, *Carbon* **129**, 847 (2018).
- [30] D. S. De, S. Saha, L. Genovese, and S. Goedecker, *Phys. Rev. A* **97**, 063401 (2018).
- [31] D. Sankar De, S. Saha, L. Genovese, and S. Goedecker, [arXiv:1802.03763](https://arxiv.org/abs/1802.03763).
- [32] S. Saha, L. Genovese, and S. Goedecker, *Sci. Rep.* **7**, 7618 (2017).
- [33] H. D. Tran, M. Amsler, S. Botti, M. A. L. Marques, and S. Goedecker, *J. Chem. Phys.* **140**, 124708 (2014).
- [34] M. Amsler, J. A. Flores-Livas, T. D. Huan, S. Botti, M. A. L. Marques, and S. Goedecker, *Phys. Rev. Lett.* **108**, 205505 (2012).
- [35] J. A. Flores-Livas, D. Tomerini, M. Amsler, A. Boziki, U. Rothlisberger, and S. Goedecker, *Phys. Rev. Mater.* **2**, 085201 (2018).
- [36] B. Schaefer, S. Mohr, M. Amsler, and S. Goedecker, *J. Chem. Phys.* **140**, 214102 (2014).
- [37] B. Schaefer, S. Alireza Ghasemi, S. Roy, and S. Goedecker, *J. Chem. Phys.* **142**, 034112 (2015).
- [38] E. W. Dijkstra, *Numer. Math.* **1**, 269 (1959).
- [39] M. Miller, D. Wales, and V. de Souza, disconnectionDPS: Fortran program to generate disconnectivity graphs from stationary point databases, <http://www-wales.ch.cam.ac.uk/software.html>.
- [40] D. S. De, M. Krummenacher, B. Schaefer, and S. Goedecker, *Phys. Rev. Lett.* **123**, 206102 (2019).
- [41] B. Schaefer and S. Goedecker, *J. Chem. Phys.* **145**, 034101 (2016).
- [42] A. Sadeghi, S. A. Ghasemi, B. Schaefer, S. Mohr, M. A. Lill, and S. Goedecker, *J. Chem. Phys.* **139**, 184118 (2013).
- [43] S. De, B. Schaefer, A. Sadeghi, M. Sicher, D. G. Kanhere, and S. Goedecker, *Phys. Rev. Lett.* **112**, 083401 (2014).
- [44] A. Stone and D. Wales, *Chem. Phys. Lett.* **128**, 501 (1986).
- [45] I. László, *Europhys. Lett.* **44**, 741 (1998).
- [46] F. Pietrucci and W. Andreoni, *J. Chem. Theory Comput.* **10**, 913 (2014).
- [47] D. Wales, *Energy Landscapes: Applications to Clusters, Biomolecules and Glasses* (Cambridge University Press, Cambridge, England, 2003).
- [48] S. G. Kim and D. Tománek, *Phys. Rev. Lett.* **72**, 2418 (1994).
- [49] S. Krishnamurty, K. Joshi, D. G. Kanhere, and S. A. Blundell, *Phys. Rev. B* **73**, 045419 (2006).
- [50] G. A. Rechtsteiner, O. Hampe, and M. F. Jarrold, *J. Phys. Chem. B* **105**, 4188 (2001).
- [51] E. Kaxiras and K. Jackson, *Phys. Rev. Lett.* **71**, 727 (1993).
- [52] R. Zwanzig, A. Szabo, and B. Bagchi, *Proc. Natl. Acad. Sci. USA* **89**, 20 (1992).
- [53] J. Tillmann, J. H. Wender, U. Bahr, M. Bolte, H.-W. Lerner, M. C. Holthausen, and M. Wagner, *Angew. Chem., Int. Ed.* **54**, 5429 (2015).
- [54] A. K. Dunker, J. D. Lawson, C. J. Brown, R. M. Williams, P. Romero, J. S. Oh, C. J. Oldfield, A. M. Campen, C. M. Ratliff, K. W. Hipps *et al.*, *J. Mol. Graphics Modell.* **19**, 26 (2001).
- [55] A. R. Oganov, C. J. Pickard, Q. Zhu, and R. J. Needs, *Nat. Rev. Mater.* **4**, 331 (2019).
- [56] <http://scicore.unibas.ch/>